Accepted Manuscript

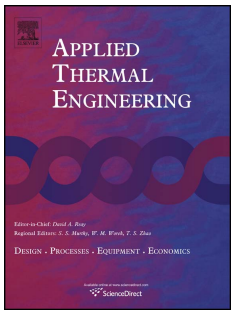

Title: Computer modelling of the laser ablation of polymers

Authors: Bálint Sinkovics, Péter Gordon, Gábor Harsányi

PII: S1359-4311(10)00269-3

DOI: 10.1016/j.applthermaleng.2010.06.022

Reference: ATE 3153

To appear in: *Applied Thermal Engineering*

Received Date: 27 October 2009

Revised Date: 25 May 2010

Accepted Date: 23 June 2010

Please cite this article as: B Sinkovics, P Gordon, G Harsányi. Computer modelling of the laser ablation of polymers, Applied Thermal Engineering (2010), doi: 10.1016/j.applthermaleng.2010.06.022

This is a PDF file of an unedited manuscript that has been accepted for publication. As a service to our customers we are providing this early version of the manuscript. The manuscript will undergo copyediting, typesetting, and review of the resulting proof before it is published in its final form. Please note that during the production process errors may be discovered which could affect the content, and all legal disclaimers that apply to the journal pertain.

ACCEPTED MANUSCRIPT

Computer modelling of the laser ablation of polymers

Bálint SINKOVICS, Péter GORDON, Gábor HARSÁNYI
Department of Electronics Technology,
Budapest University of Technology and Economics, Budapest, Hungary,
1111 Budapest, Goldmann Gy. t. 3., building V2
Phone: +36 1 463 2740, Fax: +36 1 463 4118
sinkovics@ett.bme.hu

Abstract

Laser ablation of polymers has been the subject of extensive studies for nearly three decades. Results of these investigations have shown that thermal effects play an important role during frequency tripled nanosecond Nd:YAG laser ablation of polyimide. Despite of the studies, effect of these processes has not been satisfactorily clarified. Thermal effects, photochemical and other phenomena still exist and so the thermal modelling of laser ablation is a very specialised problem. The investigation in this paper deals with special conditions in thermal models, which highly differ from more common conditions. Although there are numerous excellent thermal modelling software available, mainly in the field of electronics technology, these are not suitable or ready for handling special conditions, for example the removing of material from the domain under investigation, which is one of the most important areas. Hence we decided to develop a special thermal modelling tool. The model designing aspects which define the development process are presented in this paper.

Keywords: ablation of polyimide, laser ablation, thermal modelling

1. Introduction

Despite of the wide use of laser technologies, interaction between the laser beam and materials has not been clarified in every detail so far, especially in the case of polymers [1], [2]. Research results have shown that laser-material interaction is photothermal in the IR and photochemical in the deep UV region. In the case of polyimide thermal effects are pronounced in the ablation process [3]. However, experiments in this field have shown that thermal and chemical effects appear at the same time, and many other physical phenomena also play important role.

In electronics technology the use of laser processing is very widespread and is gaining more and more importance due to the miniaturisation. In manufacturing, applied laser parameters (pulse energy, pulse repetition frequency, speed of the moving laser spot) are adjusted to the proper value usually heuristically depending on the work in progress. The main reason for using this approach is in connection with thermal effects appearing during the laser processing. Since etch rate of the laser depends on temperature, the material structure of the sample and accumulation of heat influences etch rate. In consequence, to control the laser processing, thermal distribution of the sample has to be determined, which can be made by thermal modelling of the laser ablation. By using such modelling tool, proper laser parameters can be determined easier and faster.

Nowadays, several excellent and usable 2D and 3D thermal simulation tools are available, but usually these are specialized in general thermal problems. Capabilities of the most important types of software tools are also examined, but thermal modelling of the laser process is a very special application. Among others geometry of the domain under investigation varies during the simulation, because laser shots remove material from the sample. This one condition alone precludes the possibility of applying general thermal simulation software.

The reasons mentioned above led to the development of a special thermal modelling tool. Thermal models for modelling laser ablation have already been presented in our previous works on the subject [4]. However, in this paper we present a considerably improved modelling tool which is capable of handling non-uniform mesh and capable of applying real, measured laser beam distribution to each of the simulations.

Our software has been developed by Matlab. This solution is not optimal from the viewpoint of time consumption of the simulation, because there are faster algorithms exist, e.g. the Sincos transformation and many others [5], [6], [7]. However time consumption of simulations was acceptable for our purposes.

1.1. Basic theory for modelling of laser ablation

Final goal of our work is to obtain a model for the laser ablation which can be built into the control software of a laser micromachining system. For this reason, our model approaches the laser-material interaction from a phenomenological viewpoint and does not deal with molecular details of the process.

Generally, there are two types of approaches to laser processing models in relevant literature, one of them deals with atomic level of the processes. Aim of our models is to clarify the role of different physical phenomena in the laser-material interaction. These models also study, among others, details of the photo-thermal and photo-chemical effects [8], [9], [10] [11]; plume; plasma formation and their shielding influence [12], [13], [14], [15]; appearing mechanical stresses and acoustic waves due to the explosion-like processes during the laser shot [16]; or, coupled phenomenon like the Marangoni-convection [17]. Since these models are near to the laser-material interface, they are very complex and do not deal with the influence of the overall structure of the sample, e.g. how the sample directs the heat away from the placement of the laser shot. Our other group of models deals with the overall effect of laser processing, and ignores nearly all micro-level and other factors, e.g. the shape of the laser beam or structure of the sample when made from inhomogeneous material [18], [19], [20], [23], [21], [22].

Our model is a combination of models mentioned above due to the goals we have set. To consider the inhomogenities in thermal structure of the sample and the influence of the cumulative heat, our solution deals with the thermal distribution in the whole sample, not only that near to the laser-material interface. Besides the phenomenological viewpoint, our modelling tool makes it possible to take into consideration micro-level effects, shielding of the plasma, proportion of photo-thermal and photo-chemical phenomena, or other effects.

Essence of our solution is that energy of the laser shot is transformed into heat in the model and all necessary calculations are performed with the aim of thermal distribution [4]. As our model does not deal with the details of different phenomena arising during the very short time of the shot itself, the transformation of the energy is calculated with no time consumption.

2. Theoretical background of the thermal cell method [24]

Principle of the thermal cell method is that cells are defined in the geometry, and temperature of those cells scrutinized. Cells are considered as infinitesimal objects located in the geometric centre of elements with finite volume. Thermal resistance between the cells are provided by the geometry of finite-volume elements and the thermal parameters of materials. Those parameters also determine thermal capacitance assigned to each cell. The illustration of thermal cells can be seen in Figure 1.

Thermal resistance between cells is calculated by the thermal Ohm's law (following equations represent one-dimensional case):

$$R = \frac{x}{\lambda \cdot A} \tag{1}$$

where R is thermal resistance, x is the distance between two cells, λ is the coefficient of thermal conductivity and A is the surface, which heat flux flows through. If thermal resistance is given, then the heat flux flowing between two cells is:

$$Q_n = \frac{T_n - T_{n+1}}{R} \tag{2}$$

where T_n is the temperature of the n^{th} cell.

In the case where values of thermal resistance and capacitance assigned to cells are given, temperature of a cell in function of time can be calculated by the Taylor expansion of $T_n(t+dt)$:

$$T_n(t+dt) = T_n(t) + \frac{T_n'}{1!}(t)dt + \frac{T_n''}{2!}(t)(dt)^2 + \ldots \tag{3}$$

The first derivative of the temperature can be originated from the energy balance equation of the cell:

$$T_n(t) = \frac{1}{C_n}\int_0^t Q_n dt \tag{4}$$

where C_n is the thermal capacitance of the n^{th} cell:

$$C_n = c \cdot \rho \cdot V \tag{5}$$

where c is the specific heat capacity, ρ is the density and *V* is the volume of the element. In equation (3) the higher order terms can be neglected, since we hold the value of the time step small, so the temperature of a cell in function of time can be approximated as:

$$T_n(t+dt) = T_n(t) + \frac{Q_n}{C_n} dt \tag{6}$$

Heat loss has to be considered in the cells on the boundary of the range. In heat flux calculations the Newton formula (7) or the Stefan-Boltzmann law (8) apply:

$$Q_c = h \cdot A \cdot (T_a - T_n) \tag{7}$$

$$Q_r = \varepsilon \cdot \sigma_0 \cdot A \cdot T_n^4 \tag{8}$$

where *h* is the heat transfer coefficient, ε is the emissivity, σ_0 is the black body constant and T_a is the temperature of the gas or liquid.

3. Description of light energy transformation to heat

Energy density and fluence distribution of a Gaussian laser beam can be written as follows:

$$F(x,y,z) = F_0 \cdot e^{-\left(\frac{x^2+y^2}{2\sigma^2}+\alpha \cdot z\right)} \tag{9}$$

where α is the absorption coefficient, *x*, *y*, *z* are the space coordinates. This means that the origin is at the centre of the beam and axis z is perpendicular to the surface of the material. The first part of the exponent describes the Gaussian distribution of the laser beam and the second comes from the Lambert-Beer Law of absorption. Parameter of width (σ) comes from the "minimal spot diameter" equation:

$$4\sigma = d_{\min} = 2.44 \frac{fM^2\gamma}{D} \tag{10}$$

where d_{min} is defined as the position where the intensity drops to $1/e^2$, f is the focal distance, D is the beam diameter, M^2 is a beam quality parameter which is 1 for the TEM_{00} Gaussian beam, and γ is the wavelength [25].

To include all micro-level effects, modelling tool applies factors that determine the proportion of the beam energy transformed into heat. These factors have two well-separated roles. All effects that decrease the energy of the beam before it is absorbed by the material (i.e. plume formation, reflection, etc.) are considered in the coupling efficiency factor (CEF). Therefore, CEF is the ratio of energy coupled in the material and energy of the beam. Then energy is absorbed exponentially by the material, and transformed into heat by an efficiency factor we refer to as transform efficiency factor (TEF). TEF gives good estimation on the ratio of thermal and chemical processes that take place during the ablation process. Detailed description of how these factors are determined from real experiments was also presented in our previous work [4].

F_0 is the fluence at the centre of the beam and it can be calculated from the pulse energy (E_{imp}):

$$F_0 = \frac{CEF \cdot E_{imp}}{2\pi\sigma^2} \tag{11}$$

since the pulse energy is the definite integral of the fluence over the whole surface and it has to be decreased by CEF:

$$CEF \cdot E_{imp} = \int_{-\infty}^{\infty}\int_{-\infty}^{\infty} F_0 e^{-\frac{x^2+y^2}{2\sigma^2}} dxdy = F_0 2\pi\sigma^2 \tag{12}$$

Energy (E) in a finite element of volume (its volume is $l \times m \times n$) can be calculated based on (11):

$$E = F \cdot l \cdot m \cdot (1 - e^{-\alpha \cdot n}) \tag{13}$$

thus the rise of temperature in a finite element of volume $l \times m \times n$ can be calculated as:

$$\Delta T = \frac{TEF \cdot E}{c \cdot \rho \cdot l \cdot m \cdot n} \tag{14}$$

where *c* is the specific heat capacity, *ρ* is the density and TEF as described previously.

4. Background of the thermal modelling tool

To summarize, the main object of the Matlab-based modelling tool is to solve equation (5) considering the geometry and material parameters, the initial and boundary conditions.

The flowchart of the solution can be seen in Figure 2. At first, thermal cells and connection between cells are created according to the geometry of the domain under investigation, the output is a special descriptive structure. This step is detailed in the next section. The second step is to increase the mesh density. The third step is to create a one-dimensional temperature vector, which gives the temperature of the thermal cells. At this stage of the solution this vector is filled up with the initial temperature of the material. The next step is to calculate the effect of the laser shot according to the principles presented in section 3, this step is showing the new temperature distribution. With this knowledge and knowing the given threshold temperature, portion of material that is ablated can be determined. In the next stage, the descriptive structure has to be refreshed. Cells correspond to a piece of material which is ablated and are removed from the descriptive structure. This means that the neighbouring relations between the thermal cells have to be updated, too. In the next stage of the process, the temperature vector is re-generated according to the new descriptive structure, since the number of thermal cells is decreased due to the ablation. Thermal simulation, which determines the thermal behaviour of the domain under investigation, takes place as last step. In the case of consecutive shots, the result of the simulation refers back to the fourth step. Outputs of the whole process are temperature distribution and the surface profile.

4.1. Definition of cells and thermal connections between cells

Definition of cells and calculation of the assigned geometric parameters are completed according to the available geometric data. The domain under investigation is divided into rectangular solids and at the beginning of the process its density is constant in each direction.

Calculation, storage, determination of placing cells within the grid and relation between neighbouring cells are also important points. A descriptive structure is created by the software to handle the cells and their relationships between neighbouring cells. This is shown in expression (15).

$$\begin{bmatrix} [C_1 \quad \lambda_1 \quad x_1 \quad y_1 \quad z_1] & [C_2 \quad \lambda_2 \quad x_2 \quad y_2 \quad z_2] & \\ \underline{N_{1x+}} & \underline{N_{2x+}} & \\ \underline{N_{1x-}} & \underline{N_{2x-}} & \\ \underline{N_{1y+}} & \underline{N_{2y+}} & \\ \underline{N_{1y-}} & \underline{N_{2y-}} & \\ \underline{N_{1z+}} & \underline{N_{2z+}} & \\ \underline{N_{1z-}} & \underline{N_{2z-}} & \\ [h_{1x+} \quad h_{1x-} \quad h_{1y+} \quad h_{1y-} \quad h_{1z+} \quad h_{1z-}] & [h_{2x+} \quad h_{2x-} \quad h_{2y+} \quad h_{2y-} \quad h_{2z+} \quad h_{2z-}] & \end{bmatrix} \quad \cdots \tag{15}$$

This structure is a special two-dimensional matrix. Data in columns are assigned to the elements of a thermal cell with a given ordinal number as a row vector, so that the elements of the structure are vectors. Elements of the first row are material parameters and therefore geometric data can be assigned to the given thermal cell. These data are sequentially: C – thermal capacitance, λ – coefficient of heat conductivity, x, y and z – geometric sizes of the element. The following six rows contain the ordinals of the neighbouring cells divided into rows per direction.

If the ordinal of the n^{th} cell is included in one of the rows in the m^{th} column (in vector $\underline{N}$), it means that the n^{th} cell is the neighbour of the m^{th} cell from a specified direction, this direction defined by position of the ordinal in vector $\underline{N}$. The vector in the last row contains the coefficient of heat transfer in six directions belonging to the specified element.

4.2. Creating a system of solvable equations

If descriptive structure is made as above, a system of differential equation has to be created, according to equation (5), where the actual cell is denoted by m and its neighbours are denoted by n:

$$\frac{dT_m(t)}{dt} = \sum_{\substack{x+,x-\\y+,y-\\z+,z-}} \sum_{\underline{N_m}} \frac{T_n(t) - T_m(t)}{C_m \cdot (R^n{}_m + R_n)} \cdot dt + \sum_{\substack{x+,x-\\y+,y-\\z+,z-}} \sum_{\overline{\underline{N_m}}} h^n{}_m \cdot \frac{T^n{}_{amb}(t) - T_m(t)}{C_m \cdot R^n{}_m} \cdot dt \tag{16}$$

where $T_m(t)$ is the temperature of the m^{th} thermal cell at moment t, C_m is the thermal capacity of the m^{th} cell, $T_n(t)$ is the temperature of the neighbours of the m^{th} thermal cell selected according to the vector $\underline{N}$, $R^n{}_m$ is the thermal resistance of the m^{th} cell in the direction defined by the vectors of $\underline{N}$, R_n is the thermal resistance of the neighbouring element defined by the vector $\underline{N}$, $h^n{}_m$ is the heat transfer coefficient in the specified direction, $T^n{}_{amb}(t)$ is the ambient temperature in the direction specified. First term of the expression means that whilst the elements of the six vectors of contiguity are swept, the neighbours of the m^{th} element in the direction specified are selected and equation (2) is applied to them. The second part of the formula is applied to the elements that have no neighbours, since they are located at the boundary of the region or are in connection with an ambient atmosphere. For these cases Newton formula is used. Elements with no neighbours are denoted by $\overline{\underline{N_m}}$. Let us define multiplicators of temperature-change as follows. For the first part of the formula:

$$e_1 = \frac{1}{C_m \cdot (R^n{}_m + R_n)} \cdot dt \tag{17}$$

For the second part of the formula:

$$e_2 = \frac{h^n{}_m}{C_m \cdot R^n{}_m} \cdot dt \tag{18}$$

The definition of multiplicators in the case of neighbours in direction x is the following (direction y and z is similar):

$$e_1 = \frac{\min((y_n \cdot z_n), (y_m \cdot z_m))}{C_m \cdot \left(\frac{x_n}{2 \cdot \lambda_n} + \frac{x_m}{2 \cdot \lambda_m} \right)} \cdot dt \tag{19}$$

The numerator contains calculation of common surface of two neighbouring elements. This formula defines the surface of common side in case of both elements. The smaller value is considered by using *min()* function. It enables to define common surface of elements, even if they have only one neighbour in the specified direction. Denominator contains thermal resistance, thermal capacitance of the specified thermal cell and thermal resistance of its neighbouring element. Multiplicator regarding heat transfer is calculated as follows:

$$e_2 = \frac{h^n{}_m \cdot (y_m \cdot z_m)}{C_m \cdot \frac{x_m}{2 \cdot \lambda_m}} \cdot dt \tag{20}$$

4.3. Refreshing descriptive structure

After a laser shot, a new temperature distribution is calculated according to the cumulative heat and the energy of the shot. By knowing the new distribution, the material parts that have higher temperature, than the threshold, are ablated. In this way a new geometry is evolved. Therefore, descriptive structure has to be refreshed. Cells which have higher temperature, than the threshold, are removed from descriptive structure. For this reason, the neighbouring conditions where cells are removed have to be modified: these element no longer have neighbours in the given direction, they are instead in connection with the atmosphere.

5. Modelling of laser ablation

Modelling parameters were consistent with the parameters of the Coherent AVIA 355-4500 frequency tripled, Q-switched Nd:YAG laser system, which is the appliance used in our laser experiments. Width parameter was 6 μm, according to the laser system. Material parameters correspond to parameters of

ACCEPTED MANUSCRIPT

polyimide[1], which is a widely used polymer in electronics technology and serves as the basis of our laser-polymer investigations. Thermal parameters were the following [27]:

$$\lambda = 0.29\frac{W}{m \cdot K},\ \rho = 1470\frac{kg}{m^3},\ c = 1130\frac{J}{kg \cdot K} \tag{21}$$

According to our previous works, 0.132 TEF*CEF factor and 535 ˚C ablation threshold temperature and 1.4 $\frac{1}{\mu m}$ absorption coefficient were chosen for performing the simulation [4]. The initial temperature of the material was 25 ˚C. Initial mesh structure can be seen in Figure 3, size of mesh elements near the laser spot was 62.5 x 62.5 x 31.25 nm. For solving the time-dependent equations built-in Matlab functions (*ode()*) were used. These solvers apply adaptive time stepping, in our simulations the order of the minimal time step was 0.1 ns. Due to efficient solver algorithms, time consumption of the simulations was of the order of minutes[2] per laser shots.

The result of simulation of a single shot with 10 μJ pulse energy is presented in Figure 4, the temperature of thermal cells is shown. In Figure 4 a) thermal distribution can be observed immediately after the laser shot and the ablation. Gaussian distribution of the laser shot and gradual absorption of the energy in layers of thermal cells can be seen. Besides thermal distribution, on top of the domain under investigation the ablated hole can also be observed. In Figure 4 b) temperature of cells is presented 10 ms after the laser shot. It can be observed that thermal energy of the laser shot has spread within the material, and the material cools down due to the heat loss in the domain under investigation.

Besides temperature distribution of the domain, other output of the modelling tool is the calculated surface profile. Since the tool is capable of handling any fluence distribution, measured distribution was applied in the simulation to verify the calculated profile. Fluence distribution of the laser system was measured by scanning with a high-speed silicon photodiode[3] masked by an 5 μm pinhole[4], the fluence distribution can be seen in Figure 5. In case of investigation of one laser shot, AFM[5] micrograph of the ablation hole constituted the basis of verification for the simulation. Measured surface profile of the polyimide can be seen in Figure 6, where a single 18 μJ laser pulse was applied. Except fluence distribution, which is consistent with the measured values, applied modelling parameters are the same as in the previous case. The result of the simulation can be seen in Figure 7, where calculated surface profile in the symmetry plane of the laser beam is presented in comparison with the cross-section of the AFM micrograph. It can be seen that the simulated profile is in close proximity to the measured profile.

Consecutive shots are also simulated. Since perpendicular span of the AFM is limited, cross-section images of the polyimide foil constituted the basis of verification. In Figure 8 calculated surface profiles formed by punching can be seen. In the course of these experiments pulse repetition frequency of the laser was 30 kHz, and pulse energy was 22 μJ. By applying these parameters, considerable inhomogeneity appears in the beam, due to the frequency tripling of the laser system. Inhomogeneity can be observed in cross-section images and in simulation results as well, since the modelling tool is capable of handling the measured fluence distribution. As can be seen, simulated profiles approximate well to measured results, but it has to be noted that the modelling tool underestimates the ablated material in these experiments. The elimination of this problem requires further investigations.

6. Conclusion

A Matlab-based tool for the modelling of laser ablations of polymers from a thermal viewpoint is presented in this paper. Since the latter is a very special problem, a special approach has been applied to solving the equation of heat conduction. The finite difference method has formed the basis of the solution, a simple and expressive method. However, a novel descriptive structure has also been devised, which describes the thermal connections between the elements of the applied mesh. This descriptive structure has the following properties and abilities:

[1] Upilex-S, high temperature polyimide film, product of UBE Industries Ltd.
[2] Platform: Intel® Core™ 2 Duo 2 GHz with 2 GB of RAM
[3] Purchased from the Thorlabs GmbH, part number: FDS010
[4] Purchased from the Thorlabs GmbH, part number: P5S
[5] Veeco Innova surface probe microscope was applied in contact mode

1. Mathematical background of the solution is evident, and it can be implemented in Matlab or in other high-level programming language within a short time frame.
2. In Matlab environment, solver algorithms are already available and do not have to be implemented.
3. Due to the composition of descriptive structure, the modelling tool is capable of handling non-uniform mesh. With the use of such non-uniform mesh, accuracy of calculations is much more precise, high thermal gradient near to the laser spot can be handled easier and the time consumption of the simulation process decrease.
4. The descriptive structure makes it possible to apply further physical phenomena to take into consideration micro-level effects, such as plasma shielding or other side-effects.
5. The descriptive structure also makes it possible to handle any fluence distribution, so that real, measured distribution of the laser system can be applied in simulations.
6. The descriptive structure makes it possible to vary the geometry of the domain under investigation during the simulation.

Comparison of simulated and measured profiles of a single and multiple laser shot have been presented as verification of our method. The next phase of our work will be directed at further investigations into the application of the modelling tool.

References

[1] T. Lippert, and J. T. Dickinson: Chemical and Spectroscopic Aspects of Polymer Ablation: Special Features and Novel Directions, Chem. Rev. 103, 453-485 (2003)

[2] P.E. Dyer: Excimer laser polymer ablation: twenty years on, Appl. Phys. A 77, 167–173 (2003)

[3] T. Lippert, M. Hauer, C.R.Phipps, A. Wokaun: Fundamentals and applications of polymers designed for laser ablation, Appl. Phys. A 77, 259–264 (2003)

[4] P. Gordon, B. Balogh, B. Sinkovics: Thermal Simulation of UV Laser Ablation of Polyimide, Microelectronics Reliability, 47, pp. 347-353 (2007)

[5] V. Székely, A. Poppe, M. Rencz, M. Rosental, T. Teszéri: THERMAN: a thermal simulation tool for IC chips, microstructures and PW boards, Microelectronics Reliability, vol. 40, pp. 517-524 (2000)

[6] M. Rencz, V. Székely, A. Poppe: A fast algorithm for the layout based electro-thermal simulation, Proceedings of the Design, Automation and Test in Europe Conference and Exhibition, 03, pp. 1530-1591 (2003)

[7] Hong-Wei Song, Shao-Xia Li, Ling Zhang, Gang Yu, Liang Zhou, Jian-Song Tan: Numerical simulation of thermal loading produced by shaped high power laser onto engine parts, Applied thermal engineering 30, 553-560 (2010)

[8] E. K. Illy, D. J. W. Brown, M. J. Withford, J. A. Piper: Enhanced polymer ablation rates using high-repetition-rate ultraviolet lasers, IEEE J. Select Topics Quant Electron, 5:1543A (1999)

[9] Y. G. Yingling, B. J. Garrison: Coarse-Grained Model of the Interaction of Light with Polymeric Material: Onset of Ablation, J. Phys. Chem. 109, 16482-16489 (2005)

[10] P. F. Conforti, Y. G. Yingling, B. J. Garrison: Computational studies of ultraviolet ablation of poly(methyl methacrylate), Journal of Physics: Conference Series 59, 322–327 (2007)

[11] Y. G. Yingling, B. J. Garrison: Incorporation of chemical reactions into UV photochemical ablation of coarse-grained material, Applied Surface Science 253, 6377–6381 (2007)

[12] A. Misra, A. Mitra, R. K. Thareja: Diagnostics of laser ablated plasmas using fast photography, Applied Physics Letters, 74(7), 929–931 (1999)

[13] A. Bogaerts, Z. Chen, R. Gijbels, A. Vertes: Laser ablation for analytical sampling: what can we learn from modelling. Spectrochim. Acta, Part B 58, 1867–1893 (2003)

[14] M. I. Zeifman, B. J. Garrison, L. V. Zhigilei: Multiscale simulation of laser ablation of organic solids: evolution of the plume, Applied Surface Science 197–198, pp. 27–34, (2002)

[15] T. E. Itina, K. Gouriet, L. V. Zhigilei, S. Noel, J. Hermann, M. Sentis: Mechanisms of small clusters production by short and ultra-short laser ablation, Applied Surface Science 253, 7656–7661 (2007)

[16] M. Allmen, A. Blatter: Laser-beam interactions with materials 2nd ed., Springer (1998)

[17] Y. P. Lei, H. Murakawa, Y. W. Shi, X. Y. Li: Numerical analysis of the competetive influence of Marangoni flow and evaporation on heat surface temperature and molten pool shape in laser surface remelting, Computational Materials Science, 276-290 (2001)

[18] W. K. C. Yung, J. S. Liu, H. C. Man, T. M. Yue: 355 nm Nd:YAG laser ablation of polyimide and its thermal effect, Journal of Materials Processing Technology 101, 306–311 (2000)

[19] K. C. Yung, D. W. Zeng, T. M. Yue: XPS investigation of Upilex-S polyimide ablated by 355 nm Nd:YAG laser irradiation, Applied Surface Science 173, 193–202 (2001)

ACCEPTED MANUSCRIPT

[20] K. C. Yung, D. W. Zeng, T. M. Yue: High repetition rate effect on the chemical characteristics and composition of Upilex-S polyimide ablated by a UV Nd:YAG laser, Surface and Coatings Technology 160, 1–6. (2002)
[21] D.P. Korfiatis, K.-A.Th. Thoma, J.C. Vardaxoglou: Numerical modelling of ultrashort-pulse laser ablation of silicon, Applied surface science 255, 7605-7609 (2009)
[22] Nilanjan Chakraborty: The effects of turbulence on molten pool transport during melting and solidification processes in continuous conduction mode laser welding of copper-nickel dissimilar couple, Applied Thermal engineering 29, 3618-3631 (2009)
[23] Benxin Wu, Yung C. Shin: A simplified predictive model for high-fluence ultra-short pulsed laser ablation of semiconductors and dielectrics, Applied surface science 255, 4996-5002 (2009)
[24] D.C. Whalley: A simplified reflow soldering process model, Journal of Materials Processing Technology 150 pp. 134–144 (2004)
[25] M. S. William: Laser material processing, Springer Verlag, 58-96 (1998)
[26] P. P. Yupapin, P. Rattanathanawan: Numerical Simulation of the Three-Dimensional Heat Equation and Applications, Thammasat International Journal of Science and Technology, vol. 11, 45-51 (2006)
[27] MatWeb material database, http://www.matweb.com, 21 August 2008

ACCEPTED MANUSCRIPT

ACCEPTED MANUSCRIPT

List of figures:

Figure 1: Thermal cells

Figure 1 a): Connection of the thermal cells in the domain

Figure 1 b): Nomenclature of thermal resistances

Figure 2: A flow chart showing the most important steps in the Matlab-based modelling tool

Figure 3: Mesh structure of the domain under investigation

Figure 3 a): x-y plane, the placement of the laser spot is at the centre of this plane

Figure 3 b): x-z plane, the placement of the laser beam is in the middle-top of this plane

Figure 4: Result of simulation, temperatures of the thermal cells

Figure 4 a): Immediately after the laser shot and the ablation

Figure 4 b): After 10 ms following the laser shot

Figure 5: Fluence distribution of Coherent AVIA 355-4500 frequency tripled, Q-switched Nd:YAG laser system (pulse energy: 18 μJ)

Figure 6: AFM micrograph of ablation holes in Upilex-S, etched with one pulse of 18 μJ

Figure 7: Comparison of measured and simulated surface profiles (in the symmetry plane of the laser beam)

Figure 8: Cross-section images of polyimide foil and simulated surface profiles

Figure 8 a): after 5 shots

Figure 8 b): after 10 shots

Figure 8 c): after 15 shots

Figure 8 d): after 20 shots

ACCEPTED MANUSCRIPT

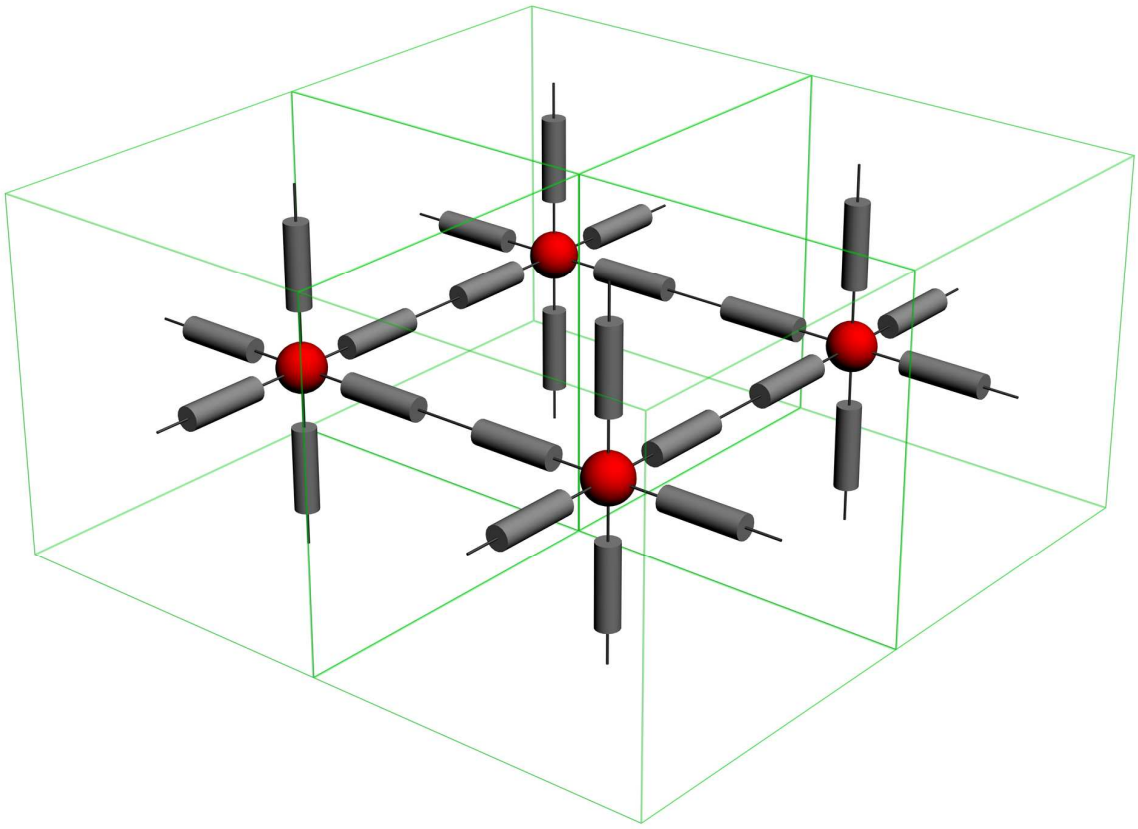

ACCEPTED MANUSCRIPT

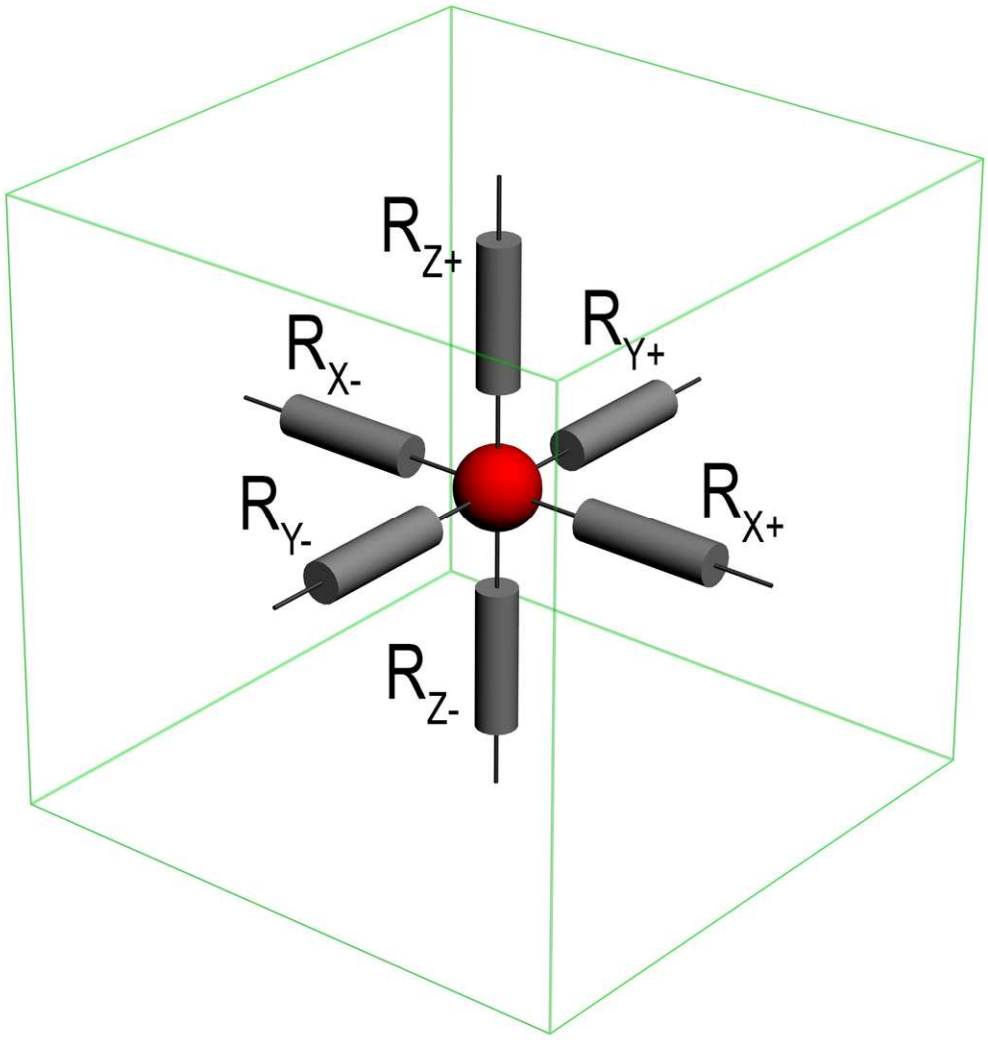

ACCEPTED MANUSCRIPT

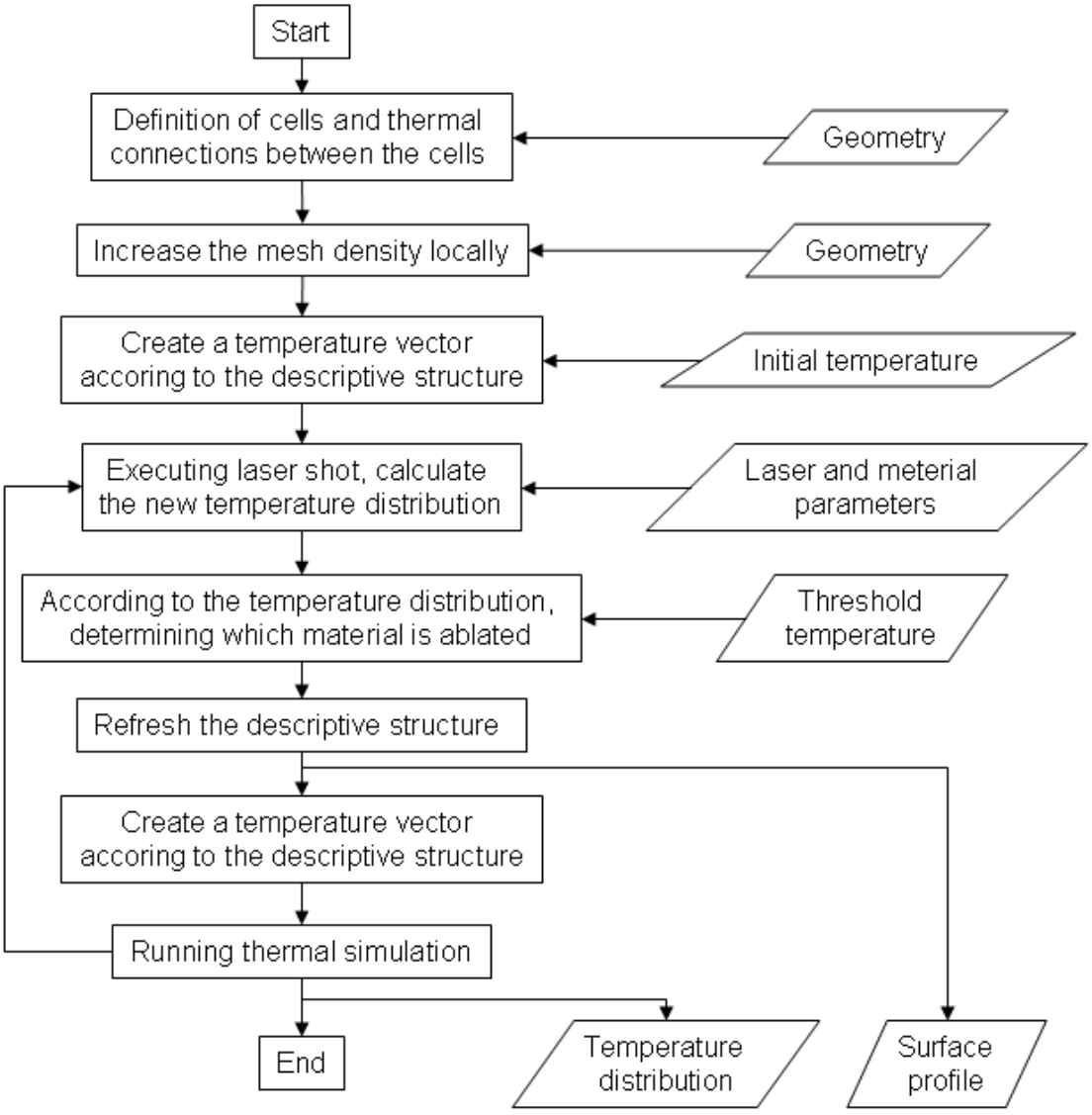
Start
Definition of cells and thermal connections between the cells
Geometry
Increase the mesh density locally
Geometry
Create a temperature vector accoring to the descriptive structure
Initial temperature
Executing laser shot, calculate the new temperature distribution
Laser and meterial parameters
According to the temperature distribution, determining which material is ablated
Threshold temperature
Refresh the descriptive structure
Create a temperature vector accoring to the descriptive structure
Running thermal simulation
End
Temperature distribution
Surface profile

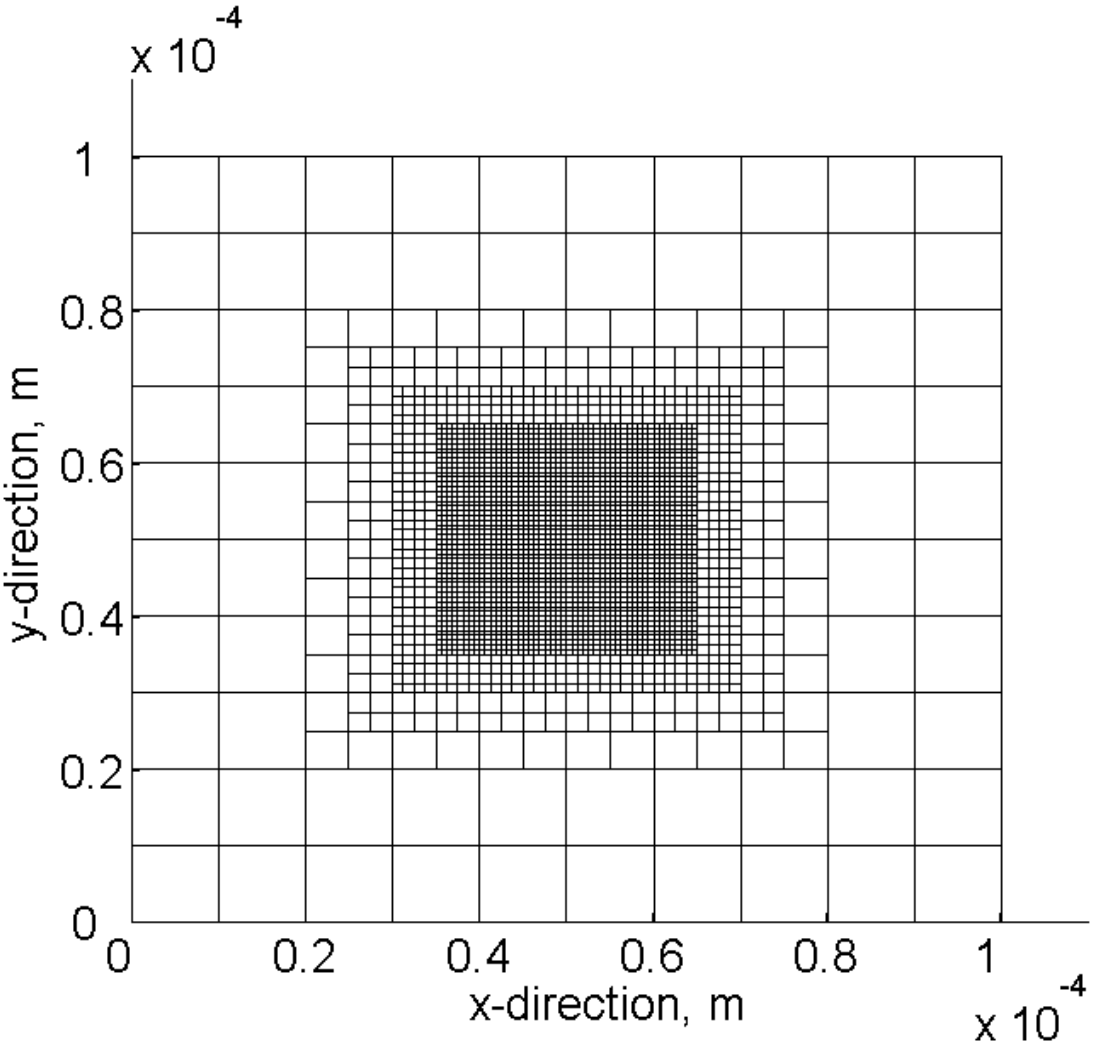
x 10^-4
1
0.8
0.6
0.4
0.2
0
y-direction, m
0
0.2
0.4
0.6
0.8
1
x-direction, m
x 10^-4

ACCEPTED

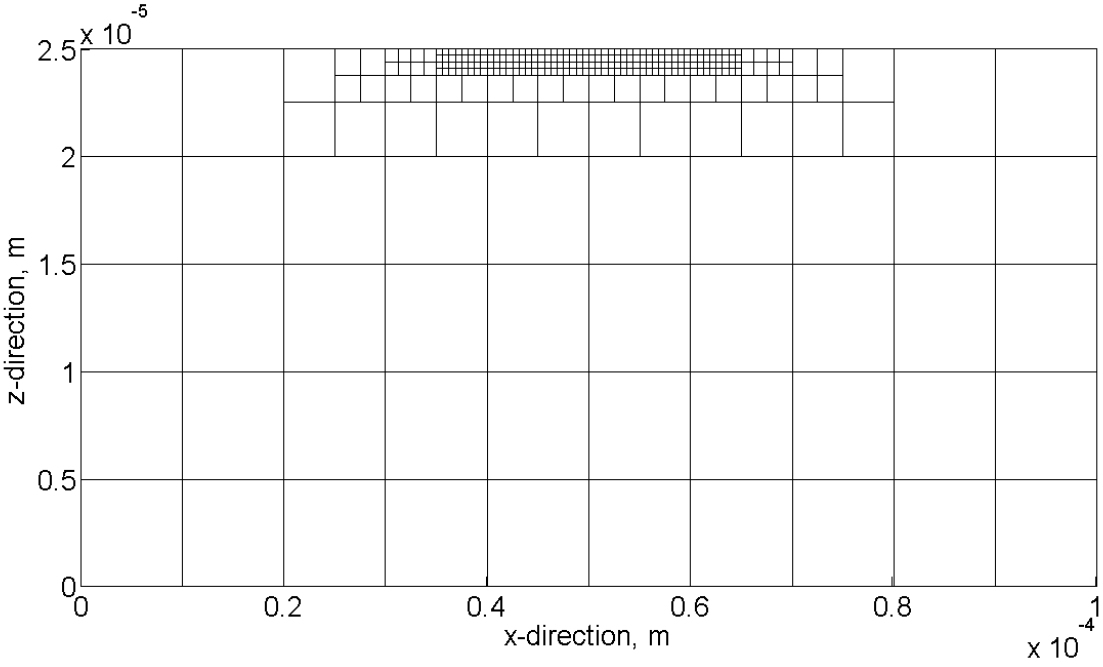

ACCEPTED MANUSCRIPT

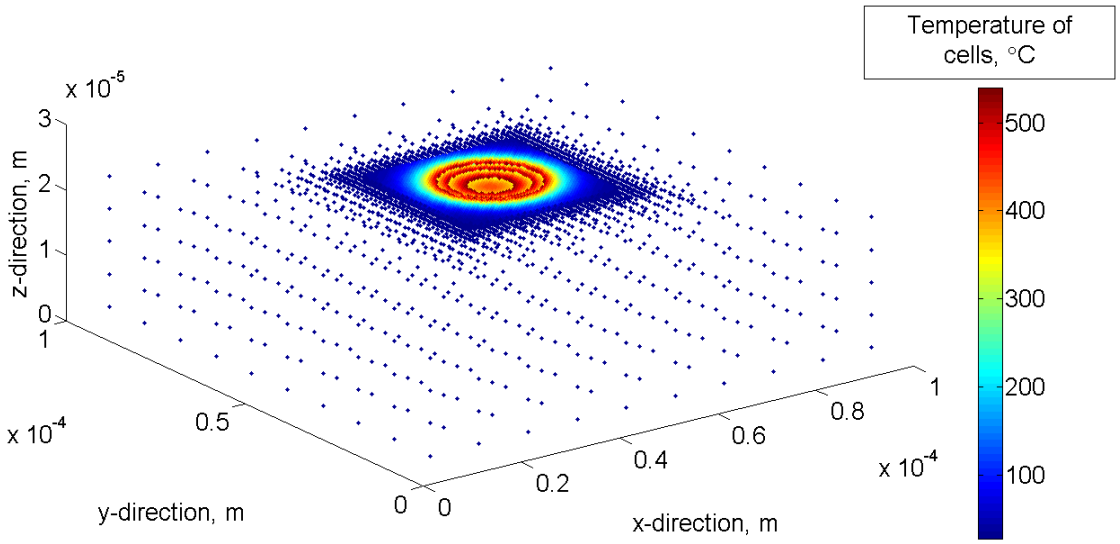

ACCEPTED MANUSCRIPT

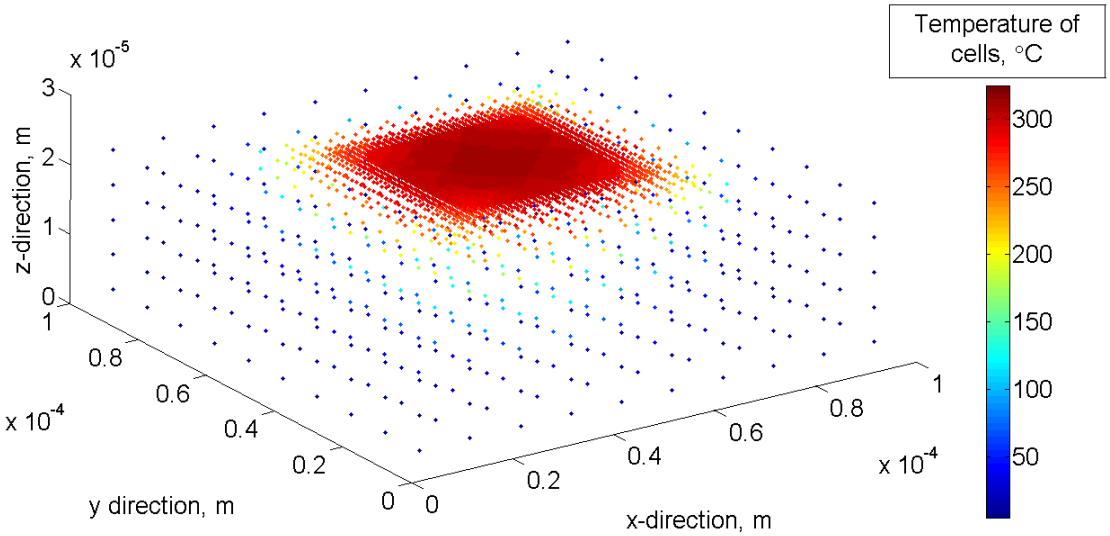

ACCEPTED MANUSCRIPT

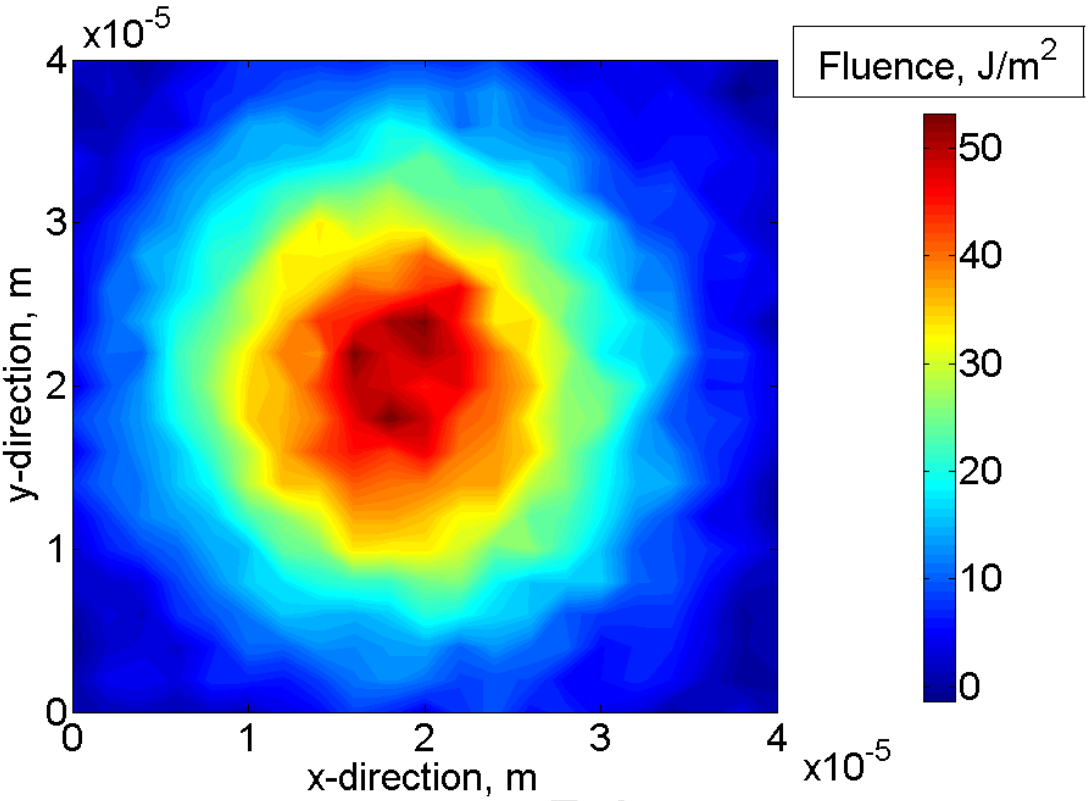

ACCEPTED MANUSCRIPT

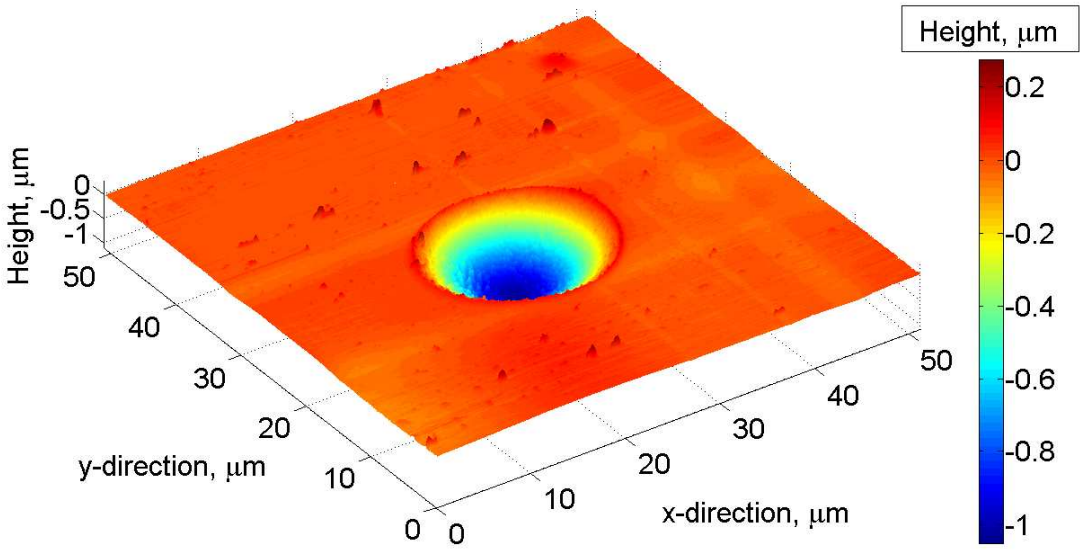

ACCEPTED MANUSCRIPT

ACCEPTED MANUSCRIPT

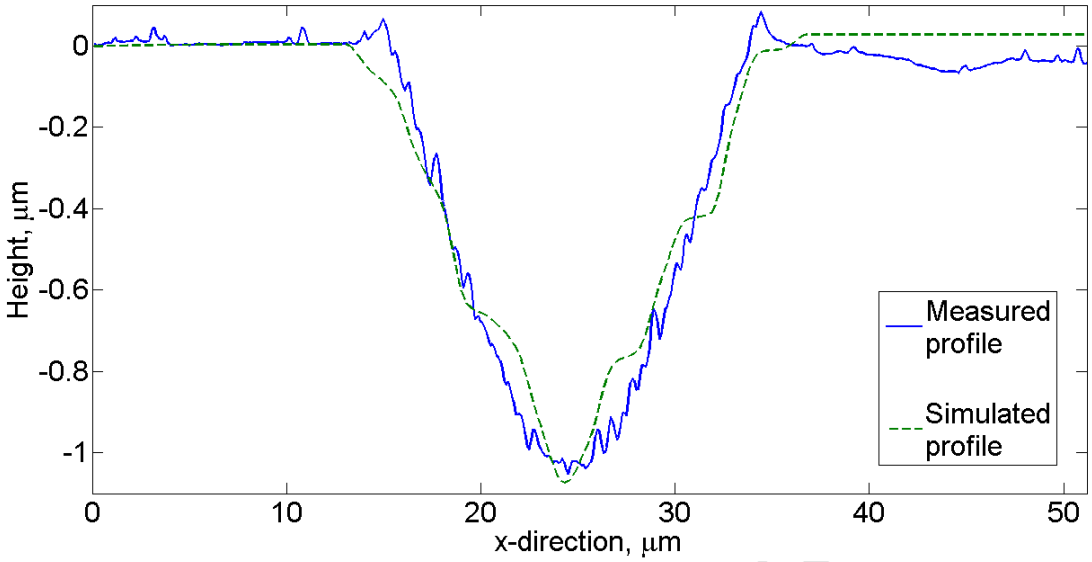

ACCEPTED MANUSCRIPT

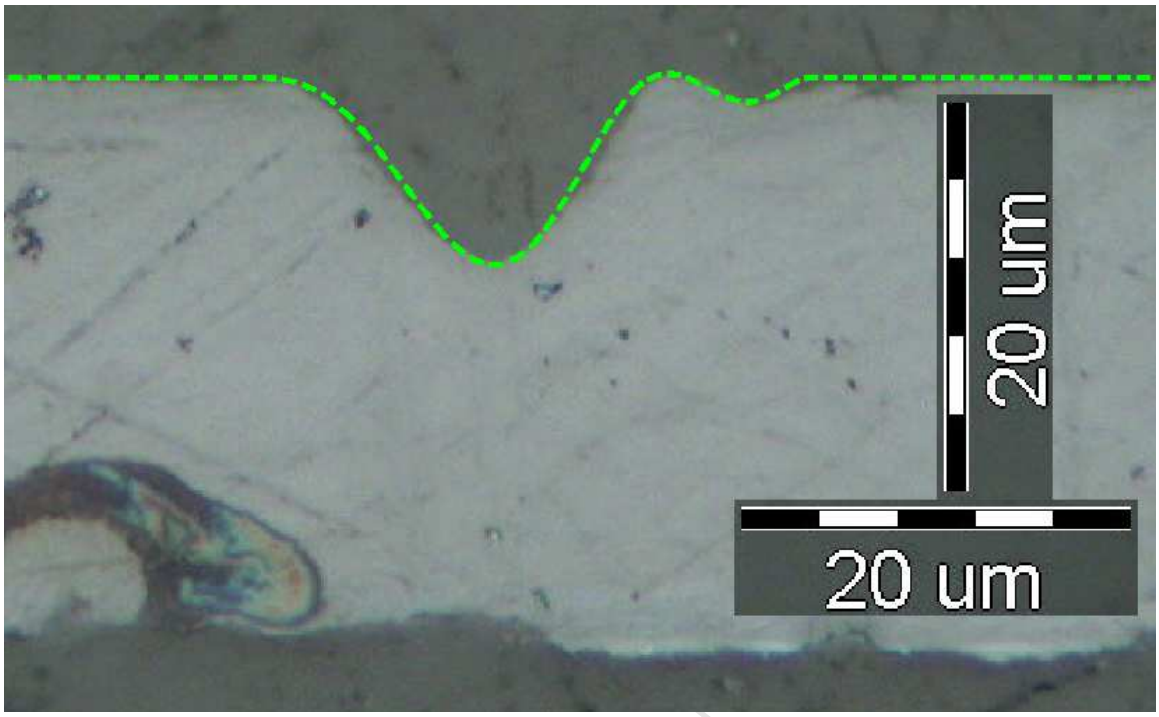

ACCEPTED MANUSCRIPT

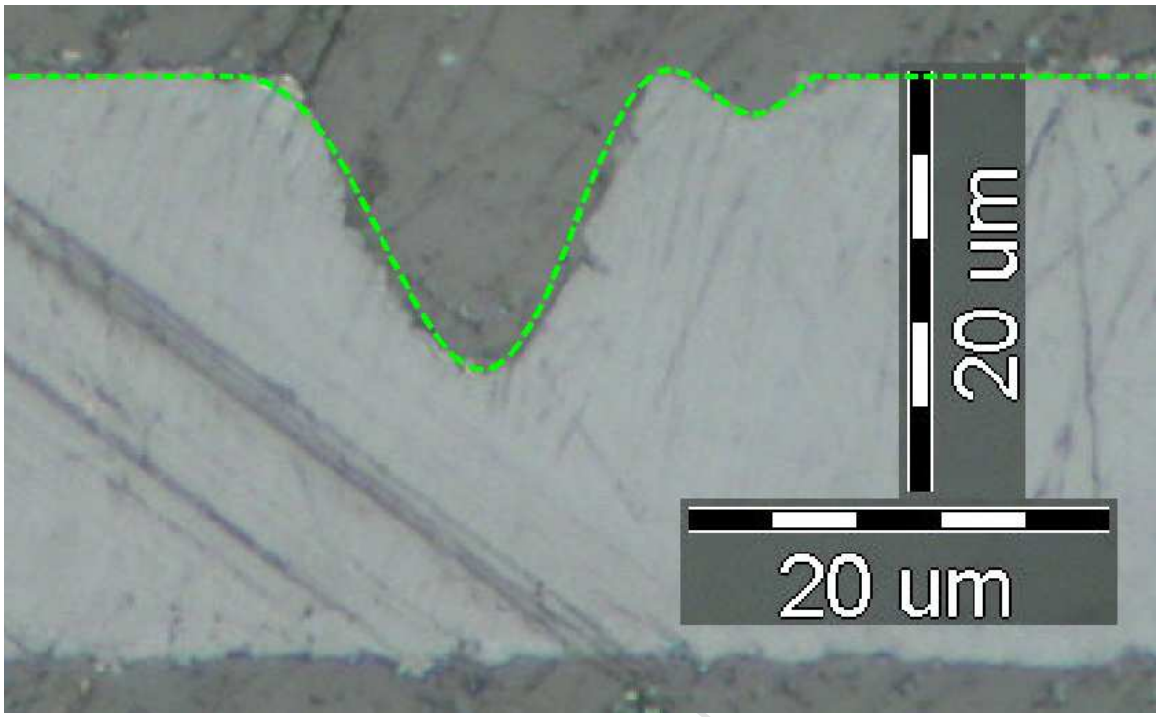

ACCEPTED MANUSCRIPT

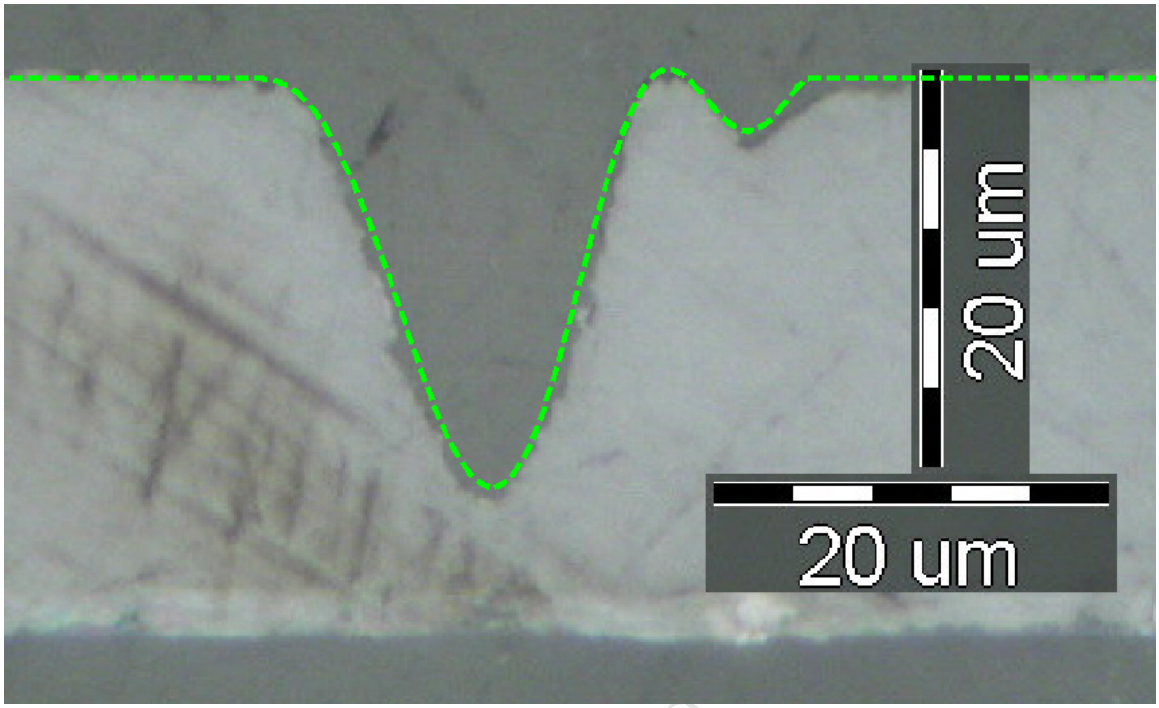

ACCEPTED MANUSCRIPT

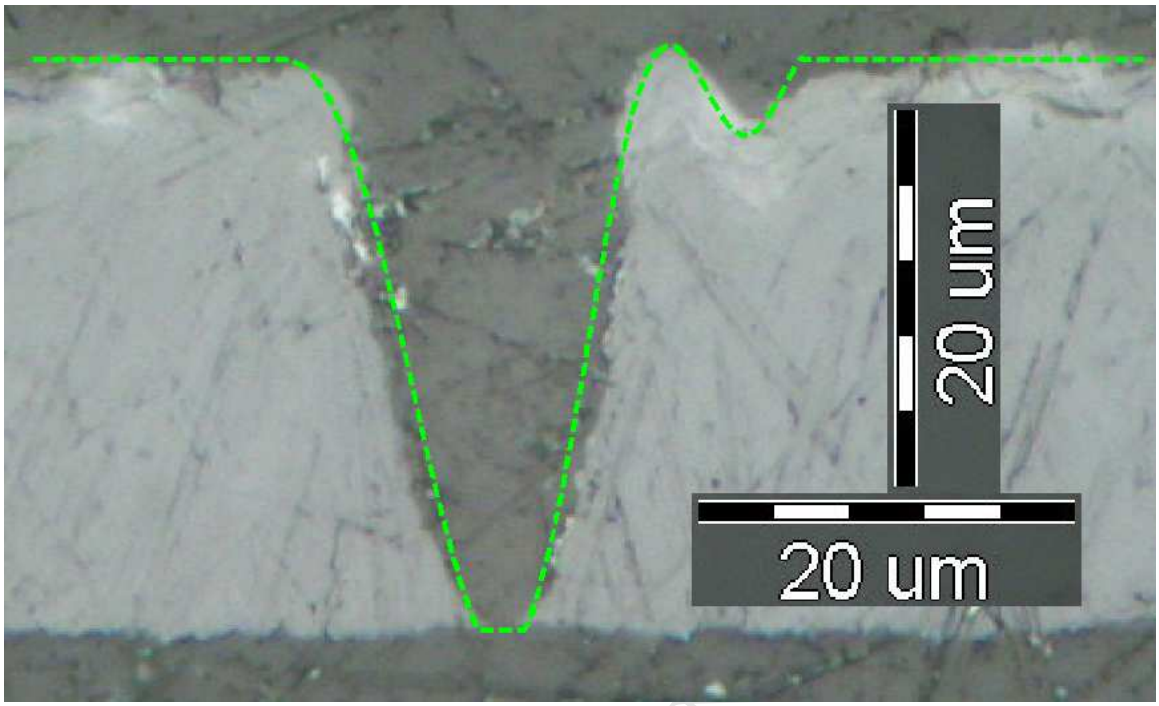

ACCEPTED MANUSCRIPT